Journal of Power Sources 193 (2009) 810–815

Contents lists available at ScienceDirect

Journal of Power Sources

journal homepage: www.elsevier.com/locate/jpowsour

Electroless-plated tin compounds on carbonaceous mixture as anode for lithium-ion battery

Yi Ruei Jhan [a], Jenq Gong Duh [a,*], Mo Hua Yang [b], Deng Tswen Shieh [b]

[a] Department of Material Science and Engineering, National Tsing Hua University, Hsinchu, Taiwan
[b] Material and Chemical Research Laboratories, Industrial Technology Research Institute, Hsinchu, Taiwan

ARTICLE INFO

Article history:
Received 8 September 2008
Received in revised form 9 March 2009
Accepted 31 March 2009
Available online 16 April 2009

Keywords:
Sn
Carbonaceous mixture
Composite anode
Electroless plating
Lithium-ion batteries

ABSTRACT

A composite anode materials was prepared that contained tin compounds of $Sn_6O_4(OH)_4$, SnO_2 and Sn_3PO_4 on the surface of carbonaceous mixture mesophase graphite particles (MGP) and nature graphite (NG). The nanosize tin compounds were electrolessly plated from aqueous solutions onto the carbonaceous mixture. The morphology and structure of tin compounds were characterized by scanning electron microscopy (SEM) and X-ray diffraction (XRD). It was found that the tin compounds particle size was a crucial factor to improve Sn compounds/Carbon composite anodes for cyclability and reversible capacity. The homogeneous dispersion and smaller particle size of tin compounds was attributed to the additive of NG. As the carbonaceous substrate was C–C mixture carbon, the particle size of Sn compounds was about 20–30 nm. However, the particle size was 100–200 nm, as the carbon substrate was singular MGP. Electrochemical performance test of the Sn compounds/C–C composite electrode shows the maximum specific charge capacity of 583 mAh g^{-1} at the 5th cycle. The charge capacity retention of Sn compounds/C–C electrode was 85% after 20 cycles. The reversible capacity of Sn compounds/C–C electrode increased 292 and 97 mAh g^{-1} more than pristine (NG + MGP) electrode and Sn compounds/C electrode at the 5th cycle, respectively.

1. Introduction

Carbonaceous compounds are widely used in commercial Li-ion batteries owing to its low potential plateau, acceptable capacity and low cost. However, carbon only exhibits a theoretical capacity of 372 mAh g^{-1} after being lithiated to form LiC_6. For the further improvement of lithium-ion batteries, the development of alternative anode materials, which possess larger capacities is required. In recent studies, binary lithium alloy systems, such as Li–Si or Li–Sn systems, have been investigated for the development of new anode materials with high capacities [1–9]. The Li–Sn system has a possibility of achieving high capacities up to 994 mAh g^{-1}, since alloys with the maximum lithium content can be formed in the system of ($Li_{4.4}Sn$) [1–4]. Nevertheless, these materials have a serious drawback when used as the anode, which is the pulverization of tin caused by its volume expansion/shrinkage during lithium-ion insertion/extraction. Recently, it was demonstrated that combining ductile carbonaceous materials with the Sn-based compounds could effectively improve the cycling stability [10].

There are several ways to synthesize the Sn compounds/carbonaceous composite anode materials. Kim et al. infiltrated tetraethyltin into mechanically milled polystyrene resin powders [11]. Jung et al. reported that spherical Sn-carbon core-shell powder was synthesized through a resorcinol formaldehyde microemulsion polymerization performed in the presence of hydrophobized Sn nano-particle followed by pyrolysis [12]. He and co-workers prepared Sn/C microsphere by adding SnO_2 powder to the water during the inverse emulsion curing of phenolic resin, followed by carbonization and carbothermal reduction of Sn in Ar atmosphere at 900 °C [13].

However, the composites of Sn/C synthesized by mechanical milling might cause the aggregation of Sn particle, therefore it could not reduce the particle size of Sn particle. In addition, lots of the energy was consumed in the process of heat treatment, and the resorcinol–formaldehyde microemulsion polymerization material used in the synthesis of Sn-carbon core-shell was expensive. As a result, the process of carbonization heat treated at 1000 °C for 1 h was a costly method to synthesize the core-shell Sn/C material.

To improve the electrochemical performance of lithium-ion battery, besides the above mentioned Sn compounds composites materials, the modification of carbon materials was also investigated. Takamura et al. tried to load nature graphite (NG), acetylene black (AB) and Ketjen black (KB) onto the active material mesophase

* Corresponding author. Tel.: +886 3 5712686; fax: +886 3 5712686.
E-mail address: jgd@mx.nthu.edu.tw (J.G. Duh).

0378-7753/$ – see front matter.
doi:10.1016/j.jpowsour.2009.03.072

carbon fiber (MCF), and claimed that incorporation of the conductive additive was quite effective to improve not only the cycle life, but also the rate of the electrochemical reaction. It was also found that the initial irreversible capacity of MCF was suppressed to a great extent. [14]. Hossain et al. [15] mentioned that carbon–carbon (C–C) composite offered many advantages, such as: high reversible capacity, no dissolution of substrate during over charge, acting as lithium-ion sink during over charge. However, the reversible capacity was still limited.

In this study, to enhance the reversible capacity of carbon electrode and the cycling stability of Sn/C composite electrodes, an inexpensive method of electroless plating was adopted to synthesize the Sn/C–C (MGP-NG) composite anode materials. This method was recently adopted by Fang et al. [16]. In this study, it was aimed that the particle size distribution and Sn compounds particle size of the as-prepared electrode could be improve by the modified plating procedure. Sn compounds/C composites and carbon–carbon mixture were combined with the electroless plating Sn compounds on the C–C (MGP-NG) mixture powders. The objective was to acquire the high lithium storage capacity of the element Sn and the stable cyclability of C–C mixture carbon. Furthermore, electroless plating was an efficient method to produce multiple phases of nanosize tin compounds simultaneously. These multiple phases were expected to act as buffers in avoiding aggregation of Sn during cycling. It was hoped that as-obtained Sn compounds/C–C composite materials would be demonstrated, showing a remarkable cycling performance and a higher reversible capacity.

2. Experimental

2.1. Preparation of Sn compounds/C, C–C composite powders

Composites of carbonaceous materials and Sn-based compounds were prepared by a modified electroless plating process. The starting reagent contained tin sulfate ($SnSO_4$, 99%), sodium hypophosphite ($NaH_2PO_2{\cdot}H_2O$, 95%) and sodium succinate hexahydrate ($Na_2C_4H_4O_4{\cdot}6H_2O$, 95%). The carbonaceous matrix included mesophase graphite powders (MGP) and mesophase graphite powders-nature graphite (MGP-NG) composite powders. Firstly, appropriate amount of $SnSO_4$ was dissolved in de-ionized water, mixed to obtain the metal-precursor. The carbonaceous powders were mixed with the reduction agent solution and then added into the precursor under strong stirring. The reaction temperature of water bath was maintained in 80 °C for 40 min. The pH value of electroless plating solution was also kept to be around 6. After electroless deposition, the obtained Sn-containing composite powders were repeatedly washed with de-ionized water until the pH value approached 7 and then dried at room temperature in vacuum.

2.2. Materials characterizations

Sn and P contents in the composites were determined by the inductively coupled plasma-atomic emission spectrometer (ICP-AES). The phase identification of derived anode materials was carried out by X-ray diffraction (XRD) operated at 40 kV and 30 mA from 10° to 80° with a wavelength of λ =1.5405 Å for CuKα. Surface morphology of Sn-containing composite anode materials was observed using a field-emission scanning electron microscope (FESEM, JSM-6500F) with a controlled accelerating voltage at 15 kV.

2.3. Electrochemical characterization

The electrochemical performance of the Sn-coating composite negative electrode was examined by two-electrode test cells consisted of the composite electrode, metallic lithium electrode, polypropylene separator and an electrolyte composed of 1 M LiPF6 in EC/EMC (1:2 vol.%) for 2032 coin cells. The composite electrode was prepared by coating the ball-milled slurry comprised of Sn-containing composite materials (95 wt.%) and PVDF binder (5 wt.%) on an cooper foil, followed by drying the coated electrode at 100 °C for 12 h in vacuum and then by roll-pressing the derived electrode. The assembled cells were galvanostatically cycled at the rate of 0.1 C between 0.001 V and 1.5 V.

3. Results and discussion

3.1. The cyclability of pristine carbon

Fig. 1 shows the cyclability of bare MGP, bare NG and bare composite (MGP + NG). The C–C mixture powder exhibits a larger reversible capacity and higher retention than that of bare MGP and bare NG.

3.2. Surface morphology and phase identification of Sn compounds/C, C–C composite materials

The electroless plating was adopted to deposit reactive Sn compounds on MGP (C) powder and MGP + NG (C–C) powder, with the purpose to utilize both advantages of electroless plating and carbon mixture. The surface morphology of the pristine MGP, Sn coated MGP and Sn coated was revealed by SEM, as shown in Fig. 2. It appears that the surface morphology was quite distinct among these materials.

From Fig. 2(a), the surface of bare MGP was revealed and average particle size of carbon was 10–20 μm. The SEM images of Fig. 2(b) show Sn compounds coated on MGP (C), indicating that numerous Sn compounds were dispersed on the surface of MGP by the electroless plating. The particle size distribution of Sn compounds/MGP was not uniform after electroless plating, which might be caused by the violent stir, leading to the breakage of MGP in the electroless plating procedure. Fig. 2(c) shows the surface morphology of Sn compounds coated on MGP + NG (C–C), indicating that spherical particles and flaky particles were mixed to each other.

From the high magnification of SEM images, the difference of surface morphology among pristine carbon, Sn compounds coated carbon and Sn compounds coated mixture carbon was evident. Fig. 3(a) shows the surface morphology of bare MGP. From the image of Fig. 3(b), the majority of particle size for Sn compound was 100–200 nm, and it appeared that the dispersion on the surface

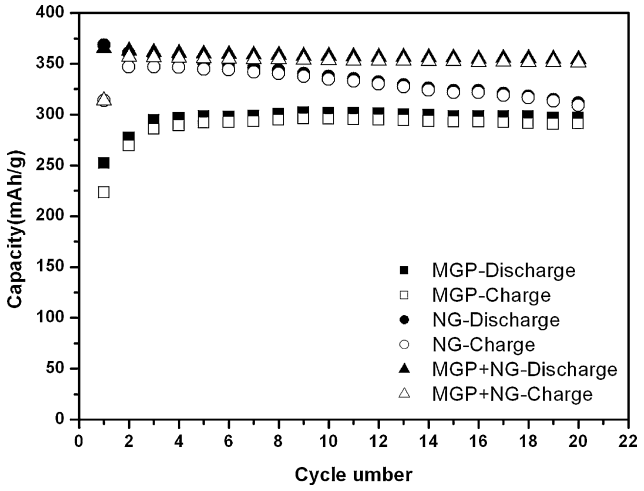

Fig. 1. Cycling performance of bare MGP, NG and MGP + NG cycled between 0.001 V and 1.5 V at 0.1 C.

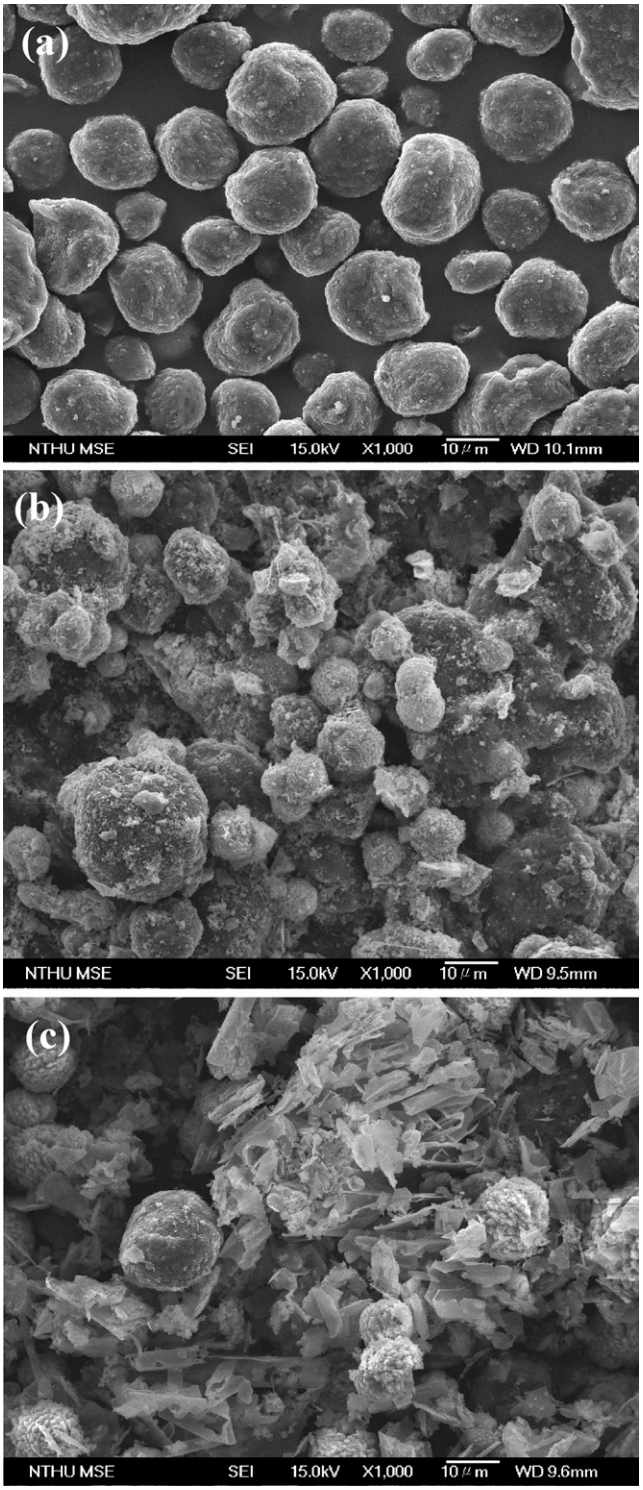

Fig. 2. SEM images of (a) Bare MGP (b) Sn compounds/MGP (c) Sn compounds/(MGP + NG).

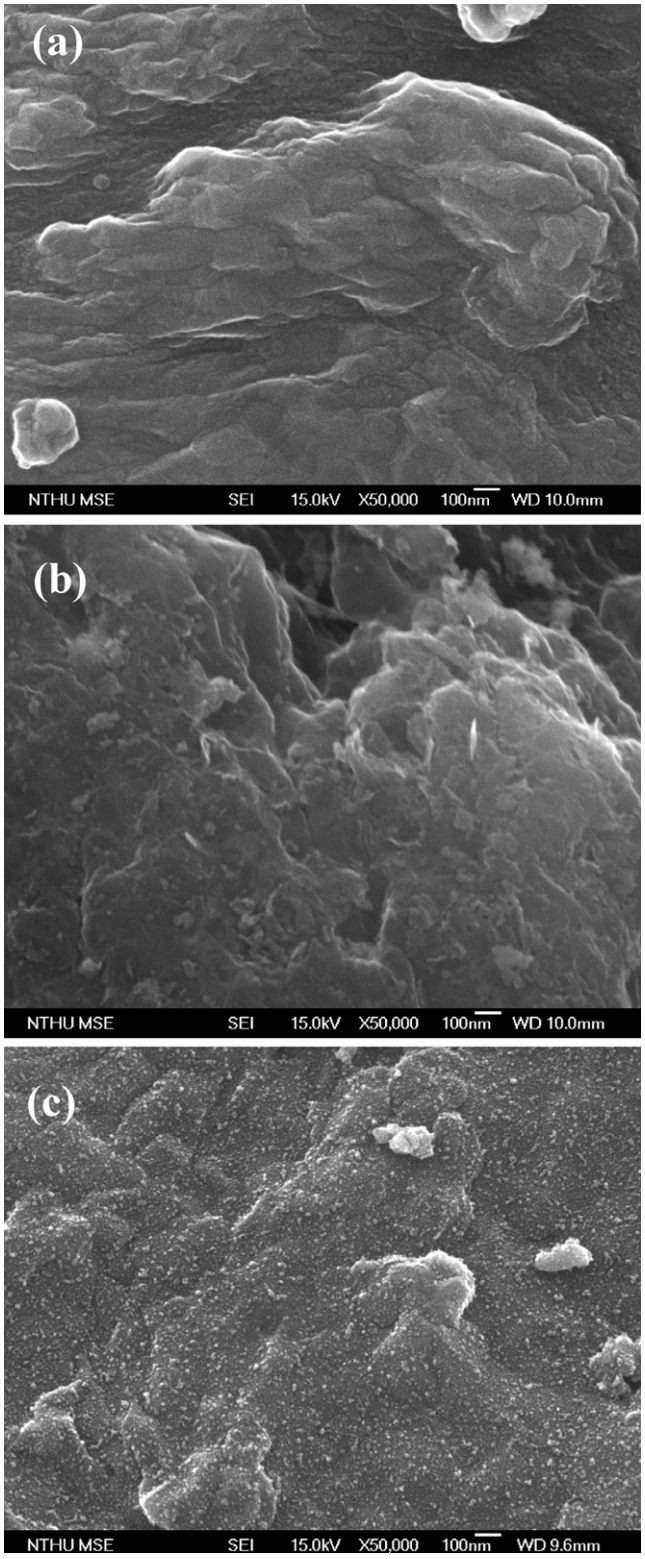

Fig. 3. Magnified SEM images of (a) Bare MGP (b) Sn compounds/MGP (c) Sn compounds/(MGP + NG).

of MGP was not uniform. However, from Fig. 3(c), a quite different image showed up. The Sn compounds were uniformly dispersed on the surface of MGP, and the particle size of Sn compounds was 10–20 nm. The reduction of size in Sn compounds was attributed to the existence of NG. Since NG has a higher surface area as indicated in Table 1, it could provide more active sites than MGP in the electroless plating. As the electroless plating was proceeded the tin ion would be adsorbed on the active site first, and then reduced by reduction agent. In addition, the presence of nature graphite could

Table 1
Surface area of bare MGP, bare NG and bare MGP + NG.

	Sample		
	MGP	NG	MGP + NG
Surface area ($m^2\ g^{-1}$)	1.4	9.3	3.8

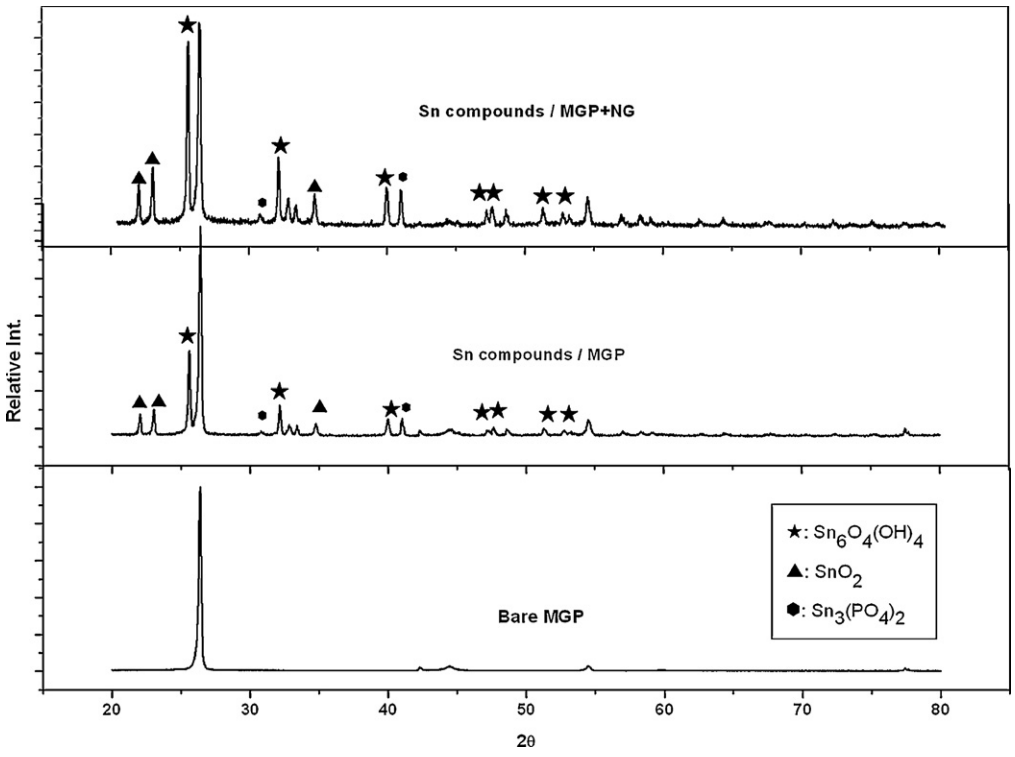

Fig. 4. X-ray diffraction pattern of the bare MGP and Sn compounds/C, C–C powders.

dilute the Sn concentration therefore it could avoid the aggregation of Sn compounds during the electroless plating.

Table 2 represents the composition of Sn compounds/C and Sn compounds/C–C electrode, which indicated that the containment of phosphate in both electrode were rare, and the contents of Sn were nearly the same under identical plating solution of electroless plating. Therefore, the composition of the electrode will not be affected by the variation of carbon content.

The XRD patterns of the composite materials shown in Fig. 4 revealed that the crystal phase were not affected by the carbon materials for identical plating solution and plating condition. The phases included $Sn_6O_4(OH)_4$, SnO_2 and $Sn_3(PO_4)_2$, which could participate in the process of Li insertion/extraction.

3.3. Electrochemical characterization of Sn compounds/C, C–C composite materials

The cycling performance of Sn compounds/C (MGP) and Sn compounds/C–C (MGP + NG) composite electrode cycled between 0.001 V and 1.5 V at 0.1 C rate (approximately 0.15 mA cm^{-2}) is shown in Fig. 5. It was apparent that the Sn compounds/C–C composite electrode exhibited superior electrochemical performance than Sn compounds/C. The irreversible capacity at the 1st cycle of Sn compounds/C–C and Sn compounds/C was 199 and 57 (mAh g^{-1}), respectively. The Sn compounds/C–C composite electrode exhibited the largest irreversible capacity, which was ascribed to the higher surface area than both the Sn compounds/C and pristine C. The surface area of MGP + NG and MGP was evaluated by BET, as listed in Table 1. The higher surface area will lead to the more solid electrolyte interface (SEI) film, and the irreversible capacity was mainly caused by SEI films. During the first four cycles, the cell was gradually activated, and the capacity was raised as shown in Table 3. The activation phenomenon was resulted from incomplete wetting of the electrode by the electrolyte. Although the 1st irreversible capacity of Sn compounds/C–C electrode was the largest, the reversible capacity and the retention after the 4th cycle were superior to the Sn compounds/C electrode. It is argued that Sn compounds with the smaller particles seem to exhibit the disadvantage of 1st irreversibility, however, it will bring about the cycling stability and increase in reversible capacity after several cycles.

Table 4 shows the charge capacity retention of the electrodes. The bare MGP electrode exhibited the highest stability among three electrodes. Its reversible capacity was, however, lower than Sn compounds/C and Sn compounds/C–C. In addition, the difference of

Table 2
ICP-AES results of Sn compounds/C and Sn compounds/C–C electrodes.

Sample	C (wt.%)	Sn (wt.%)	P (wt.%)
Sn compounds/C	63.38	36.00	0.62
Sn compounds/C–C	61.31	37.70	0.99

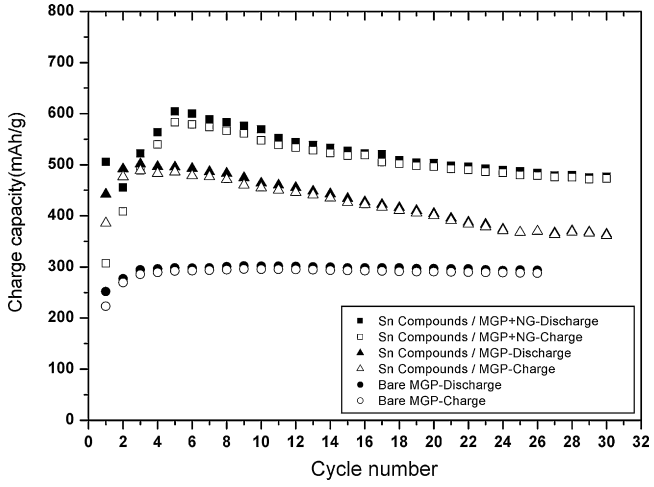

Fig. 5. Cycling performance of Sn compounds/C and Sn compounds/C–C composite materials cycled between 0.001 V and 1.5 V at 0.1 C.

Table 3
Charge capacity of bare MGP, Sn compounds/C, and Sn compounds/C–C electrodes.

Sample charge capacity (mAh g^{-1})	Bare MGP	Sn compounds/C	Sn compounds/C–C
1st	223	385	306
2nd	269	476	408
3rd	285	488	489
4th	289	483	539
5th	291	486	583
20th	290	400	496
30th	285	361	472

cycle stability between Sn compounds/C and Sn compounds/C–C became higher after long cycles. From Table 4, the effect of particle size of Sn compounds on the cycling stability was apparent.

Fig. 6 illustrates the charge and discharge curves of bare C–C, Sn compounds/C and Sn compounds/C–C between 0.001 V and 1.5 V at 0.1 C rate. Fig. 6(a) shows a voltage plateau at 0.1 V for the bare C–C electrode, which was contributed from carbon. From Fig. 6(b) and (c), the charge curve showed five distinct voltage plateaus at 0.1 V, 0.2 V, 0.4 V, 0.6 V, 0.8 V and 1 V, respectively. These voltage plateaus were contributed from carbon, $Sn_3(PO_4)_2$, $Sn_6O_4(OH)_4$ and SnO_2. Besides carbon, the voltage plateau from 0.8 V to 0.2 V corresponded to the alloying reaction of Li^+ with Sn [17]. The following equations were expected to govern the reaction of lithium with $Sn_3(PO_4)_2$ [17,18] and $Sn_6O_4(OH)_4$ [19].

$$Sn_3(PO_4)_2 + 6Li \rightarrow 2Li_3PO_4 + 3Sn \quad (1)$$

$$5Sn + Li \rightleftarrows Li_{22}Sn_5 \quad (2)$$

$$Sn_6O_4(OH)_4 + 4Li \rightarrow 4LiOH + 4SnO + 2Sn \quad (3)$$

$$LiOH + 2Li \rightarrow 2Li_2O + H_2 \quad (4)$$

$$SnO + 2Li \rightarrow Li_2O + Sn \quad (5)$$

Furthermore, the voltage plateau at 1 V was contributed from SnO_2 [20] during the process of charge/discharge reaction, which corresponded to the following equation:

$$4Li + SnO_2 \rightarrow 2Li_2O + Sn \quad (6)$$

It was observed that the capacity loss of both electrodes started from the 5th cycle. By comparing Fig. 6(b) and (c), it was revealed that Sn compounds/C electrode exhibited higher fading rate than Sn compounds/C–C electrode under voltage plateau of 0.2 V, 0.4 V, 0.6 V and 0.8 V. The difference in reversible capacity and cycling stability between Sn compounds/C and Sn compounds/C–C electrode was mainly caused by the particle size of Sn compounds. Sn compounds/C–C electrode have a smaller particle size (10–20 nm) than Sn compounds/C electrode (100–200 nm). From Eqs. (1)–(6), it was obvious that the reaction of lithium with $Sn_3(PO_4)_2$, $Sn_6O_4(OH)_4$ and SnO_2 finally produced Sn. The larger particle size of Sn compounds would lead to the more serious volume expansion. Therefore, Sn compounds/C–C electrode provided a higher cycling stability than the Sn compounds/C electrode.

For both Sn compounds/C and Sn compounds/C–C, plateau at 1.0 V indicated that the capacity fading was derived from the unavoidance of SnO_2 decomposed to Li_2O and Sn. Lithium-ion were trapped by Li_2O, leading to the formation of irreversible capacity. It was argued that the trap of lithium-ion attributed to loss of capacity was independent of particle size of Sn compounds.

Table 4
Charge capacity retention of bare MGP, Sn compounds/C, and Sn compounds/C–C electrodes after long cycle.

Capacity Retention after *n*th cycles	Bare MGP (%)	Sn compounds /C (%)	Sn compounds /C–C (%)
20th	99	82	85
30th	98	74	81

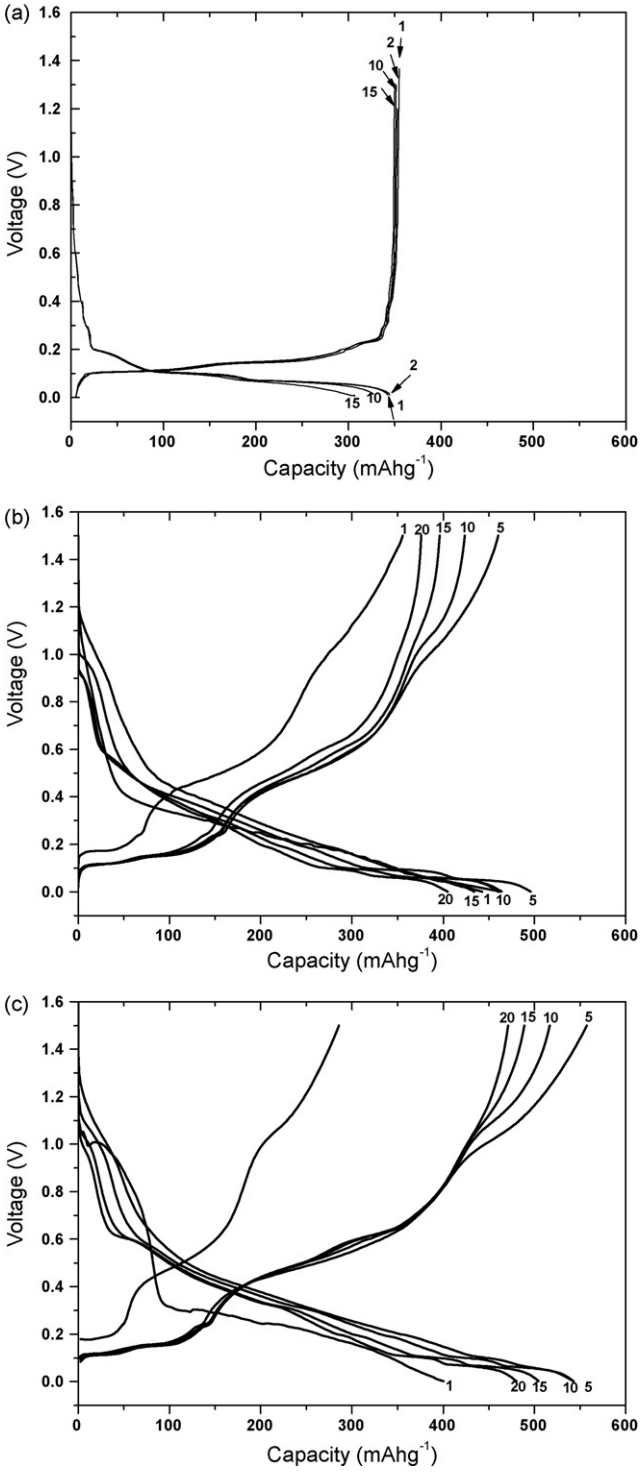

Fig. 6. Charge and discharge curves of the (a) Bare (MGP + NG) (b) Sn compounds/C (MGP) (c) Sn compounds/C–C (MGP + NG) cycled between 0.001 V and 1.5 V at 0.1 C rate.

4. Conclusions

The multi-phase of Sn compounds were synthesized by the electroless plating. The crystal phases included $Sn_6O_4(OH)_4$, SnO_2 and $Sn_3(PO_4)_2$, which could participate in Li-ion insertion and

extraction. The surface morphology of Sn compounds deposited on MGP was improved by addition of second carbon element NG. The additive NG in the electroless plating process resulted in the reduction of particle size in Sn compounds from 100–200 nm to 10–20 nm. Besides, the uniform dispersion of Sn compounds was also improved.

Owing to the modified surface morphology and Sn compounds particle size, the electrochemical performance of Sn compounds/Carbon electrode was enhanced. The 20th cycle charge capacity of the Sn compounds/Carbon (MGP + NG) electrode was 496 mAh g^{-1}, which was 96 mAh g^{-1} higher than the electrode of Sn compounds/Carbon (MGP). The retention of Sn compounds/C–C electrode and Sn compounds/C electrode was 81% and 74%, respectively, after 30 cycles.

Acknowledgements

This work was mainly supported by the Material and Chemical Research Laboratories, Industrial Technology Research Institute, Taiwan

References

[1] J. Wang, I.D. Raistrick, R.A. Huggins, J. Electrochem. Soc. 133 (1986) 457–460.
[2] Y. Idota, T. Kubota, A. Matsufuji, Y. Maekawa, T. Miyasaka, Science 276 (1997) 1395–1397.
[3] J.O. Besenhard, J. Yang, M. Winter, J. Power Sources 68 (1997) 87–90.
[4] M.M. Thackeray, J.T. Vaughey, A.J. Kahaian, K.D. Kepler, R. Benedek, Electrochem. Commun. 1 (1999) 111–115.
[5] A. Net, R.A. Huggins, W. Weppner, J. Power Sources 119–121 (2003) 95–100.
[6] H. Li, X.J. Huang, L.Q. Chen, G.W. Zhou, Z. Zhang, D.P. Yu, Solid State Ionics 135 (2000) 181–191.
[7] J. Yang, Y. Takeda, N. Imanishi, O. Yamamoto, J. Electrochem. Soc. 146 (1999) 4009–4013.
[8] J. Yang, M. Wachtler, M. Winter, J.O. Besenhard, Electrochem. Solid-State Lett. 2 (1999) 161–163.
[9] J.O. Besenhard, J. Yang, M. Winter, J. Power Sources 68 (1996) 87–90.
[10] G.X. Wang, J.-H. Ahn, M.J. Lindsay, L. Sun, D.H. Bradhurst, S.X. Dou, H.K. Liu, J. Power Sources 97–98 (2001) 211–215.
[11] S. Kim, G.E. Blomgren, P.N. Kumta, Electrochem. Solid-State Lett. 3 (2004) 44–48.
[12] Y.S. Jung, K.T. Lee, J.H. Ryu, D. Im, M. Seung, J. Electrochem. Soc. 152 (2005) 1452–1457.
[13] K. Wang, X. He, J. Ren, C. Jiang, C. Wan, Electrochem. Solid-State Lett. 7 (2006) A320–323.
[14] T. Takamura, M. Saito, A. Shimokawa, C. Nakahara, K. Sekine, S. Maeno, N. Kibayashi, J. Power Sources 90 (2000) 45–51.
[15] S. Hossain, Y. Saleh, R. Loutfy, J. Power Sources 96 (2001) 5–13.
[16] T. Fang, L.Y. Hsiao, J.G. Duh, S.R. Sheen, J. Power Sources 160 (2006) 536–541.
[17] C.M. Burba, R. Frech, J. Electrochem. Soc. 152 (2005) 1233–1240.
[18] M. Behm, J.T.S. Irvine, Electrochim. Acta 47 (2002) 1727–1738.
[19] K. Lin, X. Wang, Tsinghua Sci. Technol. 10 (2005) 554–560.
[20] Y.C. Chen, J.M. Chen, Y.H. Huang, Y.R. Lee, H.C. Shih, Surf. Coat. Technol. 202 (2007) 1313–1318.